RSC Advances



PAPER

View Article Online
View Journal | View Issue



Cite this: RSC Adv., 2024, 14, 34855

Study on the sorption and desorption behavior of La³⁺ and Bi³⁺ by bis(2-ethylhexyl)phosphate modified activated carbon†

Hongshan Zhu, ¹

Babe Stephan Heinitz, ¹

Babe Koen Binnemans, ¹

Steven Mullens ¹

and Thomas Cardinaels ¹

**Assume the stephan Heinitz, ¹

Babe Assume the stephan Heinitz, ¹

Bab Assume the stephan Heinitz, ¹

B

The separation of ²¹³Bi from its parent radionuclide ²²⁵Ac *via* radionuclide generators has proven to be a challenge due to the limited performance of the current sorbents. This study evaluated the separation performance of La³⁺ (as a surrogate for ²²⁵Ac) and Bi³⁺ using bis(2-ethylhexyl)phosphate monofunctionalized activated carbon (HDEHP/AC). The potential applications of phosphate groups as active sites and the carbon structure as a sorbent support were confirmed and validated. Various factors, including pH values, salt concentration, halide ions, contact time, solid-to-liquid ratio, initial La³⁺/Bi³⁺ concentration, and gamma irradiation were examined through batch sorption experiments in both single and binary systems. HDEHP/AC had a high sorption capacity for La³⁺ via electrostatic attraction, with the sorption data fitting well to the pseudo-second-order kinetic equation and Langmuir model. The sorption performance of La³⁺ on HDEHP/AC was minimally affected as the NaCl/NaI concentrations increased at pH = 2, whereas the sorption capacity for Bi^{3+} decreased significantly. Additionally, selective desorption of La³⁺ and Bi³⁺ was achieved using HNO₃ and Nal solutions, respectively. These results backed up by a conceptual separation process point toward a potential use of these materials in a direct/inverse ²²⁵Ac/²¹³Bi radionuclide generator. Further optimization of the material and separation process will be required to bring this class of promising materials into an actual generator for medical applications.

Received 30th August 2024 Accepted 30th September 2024

DOI: 10.1039/d4ra06276k

rsc.li/rsc-advances

1. Introduction

The short-lived radionuclide 213 Bi ($t_{1/2}=45.61$ min) has received increasing attention for targeted alpha therapy for cancer treatment due to its favorable physical and radiobiological properties. It undergoes a series of alpha- and beta-decays to the near-stable isotope 209 Bi ($t_{1/2}=1.9\times10^{19}$ years), without long-lived intermediates. Specifically, the decay of 213 Bi, with a branching ratio of 97.86%, leads to a pure alpha-emitter 213 Po ($t_{1/2}=3.708~\mu$ s), which emits high-energy alphaparticles (approximately 8 MeV). He decay of the targeted cancer cells. Currently, 213 Bi is produced directly by the decay of the relatively long-lived radionuclide 225 Ac ($t_{1/2}=9.920~days$), which can be subsequently separated by

Understanding the interactions between active sorption sites and radionuclides is a key strategy for developing alternative materials and optimizing the separation process. ^{3,12} Previous studies have shown that ²²⁵Ac³⁺ can be tightly adsorbed onto organic resins with sulfonic acid groups (*e.g.*, AG MP-50 and Dowex 50W-X8) through electrostatic attraction and ion exchange. Also, the desorption of ²¹³Bi³⁺ can be achieved by elution with halide anions (*e.g.*, I⁻ and Cl⁻). ^{13,14} However, the life-time of these materials is limited to about 1 day, due to the radiolysis-induced the scission of sulfonic acid groups and the changes in cross-linking of their macromolecular backbone. ^{9,11,13,15} Moreover, a very high concentrations of acids such as HNO₃ or HCl (*e.g.*, 8 mol L⁻¹ HNO₃) should be used to recycle

radionuclide generators. ^{1,8} However, the separation of ²¹³Bi from ²²⁵Ac occurs in harsh conditions, posing stringent requirements on the performance and life-time of the sorbents used in the generators. Despite the fact that a range of sorbents have been investigated for this application, issues of low resistance to radiolysis and poor chemical stability make the separation of medical grade ²¹³Bi in many cases a challenge. ⁹⁻¹¹ Considering these limitations, the development of alternative sorbents and the optimization of the related separation process are of great importance for the further development and implementation of targeted ²¹³Bi therapy. ⁹

^eBelgian Nuclear Research Centre (SCK CEN), Institute for Nuclear Materials Science, Boeretang 200, B-2400 Mol, Belgium

^bKU Leuven, Department of Chemistry, Celestijnenlaan 200F, P. O. Box 2404, B-3001 Leuven, Belgium. E-mail: thomas.cardinaels@kuleuven.be

Flemish Institute for Technological Research (VITO NV), Sustainable Materials Management, Boeretang 200, 2400 Mol, Belgium

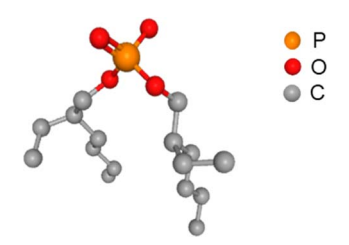
[†] Electronic supplementary information (ESI) available. See DOI: https://doi.org/10.1039/d4ra06276k

the undecayed $^{225}Ac^{3+}$ from the column due to the strong affinity of the sulfonic acid group for $^{225}Ac^{3+}$, possibly impacting the further reuse of $^{225}Ac^{3+}$.16

The sorption and desorption mechanisms of carbon materials with carboxylic groups for La³⁺/Ac³⁺/Bi³⁺ were revealed in our previous studies. These materials have shown a potential for the selective sorption performance of Bi³⁺ over La³⁺/Ac³⁺ under a low pH value (*e.g.*, pH 1-2) and a high salt concentration (*e.g.*, 2-3 mol L⁻¹ NaNO₃). Although a series desorption experiments have done to discover an eluent to selective desorption of Bi³⁺, the contamination of La³⁺/Ac³⁺ has also been eluted. Therefore, due to the lack of a suitable eluent, it remains challenging to use these materials in direct generators.

Phosphorus-containing groups, such as phosphonic, phosphoric, and phosphinic acid groups, are known for their interaction with metal ions. Sorbent materials comprising such functional groups have been extensively studied due to their affinity towards to rare earth elements and actinides ions, with high selectivity towards the hard Lewis acid cations, especially lanthanides. 17-22 Another benefit of phosphorus-containing groups is their higher radiation stability compared to sulfonic acid groups.23 One approach to synthesize such sorbents consists in the impregnation of an active phase (extractants) into a solid support.24-28 Despite the diversity in extractants and the nature of the solid support, only a few studies have systematically examined their potential use in ²²⁵Ac/²¹³Bi generators. Wu et al. explored the separation performance of actinide (AC) resin, which is composed of P,P'-di(2-ethylhexyl) methanediphosphonic acid (H2DEH[MDP]) and silica matrix, for use in direct ²²⁵Ac/²¹³Bi generators. ²⁹ However, the relatively low radiation stability of silica and H2DEH[MDP] has limited their application, together with the observation of silica leaching at a low pH.9,30,31 Furthermore, AC resin has shown a strong affinity for ²²⁵Ac even in a relatively high acidic solution, which may hinder the recycling and reuse of undecayed ²²⁵Ac³⁺ from the AC resin.21,29 Interestingly, Horwitz et al. reported that the sorption of Ac3+ onto di(2-ethylhexyl)orthophosphoric acid as the stationary phase on Celite was significantly low in $0.1~{
m mol~L^{-1}~HNO_3}$ solutions. 32 Ondrák et al. reported the use of α-ZrP-PAN composite in a direct 225 Ac/ 213 Bi radionuclide generator, achieving 213Bi yield of 77-96% in a 2.8 mL.33 The elution was performed using 10 mM DTPA. However, the detailed separation mechanism of this material was not examined. Typically, the eluent should ideally be salt, which can be easily chelated by other chelators. Ostapenko et al. also found that most La³⁺ could be eluted by 0.1 mol L⁻¹ HNO₃ solutions from Ln resin (di(2-ethylhexyl)phosphoric acid (HDEHP) immobilized onto a solid support).27 Thus, the use of phosphate/phosphoric acid functional groups is expected to be favorable for the recycling and reuse of undecayed ²²⁵Ac³⁺.

The selection of solid support for the extractants in a generator column is also critical, with high requirements on their radiolytic and chemical stability.^{26,34} Various materials have been developed as solid supports for the immobilization of extractants, such as silica, polymer resins, powdered glass, and activated carbon.^{24,26,31,35,36} Among these, activated carbon materials have shown to be particularly attractive due to their



Scheme 1 Suggested structure of HDEHP.

large surface area, high porosity, stable pore structure, and good stability.³⁷ However, experiments are still needed to explore the separation mechanism using such materials. Therefore, this study explores the use of bis(2-ethylhexyl) phosphate (Scheme 1) monofunctionalized activated carbon (HDEHP/AC) as a sorbent for the Ac³⁺ (or its surrogates)/Bi³⁺ separation. The primary focus was to demonstrate the performance of such phosphate monofunctionalized carbon surface as a model, allowing the unambiguous evaluation of the performance/influence of the phosphate group.

The physical and chemical properties of HDEHP/AC were characterized by various techniques such as scanning electron microscopy (SEM), diffuse reflectance infrared Fourier transformations (DRIFT), N₂ sorption, elemental analysis, and inductively coupled plasma optical emission spectroscopy (ICPOES). A series of batch experiments were conducted to investigate the separation behavior of HDEHP/AC for La³⁺ and Bi³⁺ under various influencing factors (*e.g.*, pH values, salt concentration, contact time, initial concentrations of metal ions, gamma-ray irradiation), and the conceptual design of ²²⁵Ac/²¹³Bi separation process was discussed. The findings of this study are expected to contribute to the development and fabrication of alternative materials for use in ²²⁵Ac/²¹³Bi radionuclide generators.

2. Experimental section

2.1. Materials and reagents

La(NO₃)₃·6H₂O (99.99%), Bi(NO₃)₃·5H₂O (98%), NaNO₃ (\geq 99.0%), and HNO₃ (\geq 65%) were purchased from Sigma-Aldrich. HCl (37%) was purchased from Fisher Scientific. NaCl (\geq 99.5%), NaOH (\geq 99.0%), and bis(2-ethylhexyl) phosphate modified activated carbon (902 470) were purchased from Merck. Milli-Q water (18.2 M Ω cm @ 25 °C) was used in the experiments. All chemicals in this study were used without further purification.

2.2. Batch sorption experiments

Stock solutions with La³⁺ and Bi³⁺ were prepared by dissolving appropriate amounts of La(NO₃)₃·6H₂O (99.99%) and Bi(NO₃)₃·5H₂O (98%) in 0.01 and 0.30 mol L⁻¹ HNO₃ solutions, respectively, to obtain a concentration of 100 mg L⁻¹ for each ion. Then, the NaOH and HNO₃ were utilized to adjust the pH values of the solutions. Batch sorption experiments were carried out in 50 mL plastic centrifuge tubes with a suitable mass of HDEHP/AC added into a 30 mL of the liquid phase. To

Paper **RSC Advances**

investigate the solid-to-liquid ratio, HDEHP/AC with different mass values was mixed with a given concentration of La³⁺ and Bi³⁺ solution (30 mL). Various concentrations of NaNO₃/NaCl/ NaI were added to examine the effect of salt concentrations and halide ions. Kinetic time was investigated by controlling the shaking time (2-180 min) in single and binary systems. Sorption isotherms were measured by increasing the initial concentrations of La3+ and Bi3+ in both single and binary systems. Except where stated otherwise, the reaction suspension was shaken at 140 rpm in a shaker for 24 hours at room temperature. The separation of sorbent from liquid phase was performed using 0.45 µm PTFE syringe filters, and the La³⁺ and Bi³⁺ concentrations in the liquid phase were measured by ICP-MS/ICP-AES.

The sorption capacity for ²²⁵Ac was also investigated by using a 30 mL liquid phase containing 100 kBq ²²⁵Ac, 10 μmol L⁻¹ La^{3+} , and 10 μ mol L^{-1} Bi^{3+} with 60 or 400 mg HDEHP/AC as the solid phase. The reaction suspension was shaken at 140 rpm for 2 hours, and the remaining steps were similar to those described above. The activities of ²²¹Fr and ²¹³Bi were measured by a high-purity germanium (HPGe, Princeton Gamma Tech) detector, while the activity of ²²⁵Ac was calculated based on the relation between ²²⁵Ac and ²²¹Fr/²¹³Bi.³⁴

2.3. Desorption experiments

The liquid solution used in the sorption process was composed of 10 μ mol L⁻¹ La³⁺, and 10 μ mol L⁻¹ Bi³⁺. Then, 400 mg of HDEHP/AC was added to the liquid solution, and the reaction suspension was shaken at 140 rpm in a shaker for 24 hours at room temperature. Afterwards, a 1.0 mL of different HNO3 solution concentrations was added into the reaction suspension, which was shaken for 24 h. Finally, the separation of sorbent from liquid was performed using 0.45 µm PTFE syringe filters, and the La³⁺ and Bi³⁺ concentrations in the liquid phase were measured by ICP-MS/ICP-AES. For the desorption process with NaI eluate, after the sorption process, 0.15-3 mL of NaI solution was added into the reaction suspension to adjust the concentration of NaI within $0.005-0.45 \text{ mol L}^{-1}$.

2.4. Stability experiments

To determine its chemical stability in an aqueous solution, dry HDEHP/AC with different mass values (e.g., 100, 200, 300, 400, and 500 mg) was immersed into 40 mL of 0.01-0.5 mol L^{-1} HNO₃ solution in a 50 mL plastic centrifuge tube, and then the plastic centrifuge tubes were shaken at 180 rpm for 150 hours. HDEHP/AC was removed using 0.45 μm PTFE membrane filters, and then the HDEHP/AC residue was dried in an oven at 70 °C. The mass weight of P for the HDEHP/AC was measured by ICP-OES.

To determine its radiation stability, the dry HDEHP/AC was placed into a glass vial and then irradiated with gamma rays from a 60 Co source (BRIGITTE, SCK CEN). The absorbed dose for HDEHP/AC was 862 \pm 121 kGv with a dose rate of 8.9 kGv h⁻¹, and its radiation stability was investigated by conducting batch sorption experiments.

2.5. Characterization

The surface morphology of HDEHP/AC was analyzed by SEM (FEI Nova NanoSEM 450), and XRD (X'Pert Pro, PAN analytical, Cu radiation source) was used to investigate the carbon structure. Elemental analysis (Vario EL and Oxy Cubes) and ICP-OES (Agilent Technologies Inc. - 5100) were performed to quantify the C, O, H, and P element amounts. The diffuse reflectance infrared Fourier transformations (DRIFT) spectroscopy (Nicolet 6700) with an in situ DRIFT accessory type 'Harrick Praying Mantis' was used to identify the surface functional groups. Thermal stability was determined by TGA (Netzsch STA 449 F3).

2.6. Data analysis

The sorption percentage R (%), sorption amount q_e (µmol g^{-1}), distribution coefficient K_d (mL g^{-1}), and desorption percentage D (%) were expressed as follows:

$$R(\%) = \frac{C_{\rm o} - C_{\rm e}}{C_{\rm o}} \times 100\% \tag{1}$$

$$R(\%) = \frac{A_{\rm o} - A_{\rm e}}{A_{\rm o}} \times 100\% \tag{2}$$

$$K_{\rm d} = \frac{C_{\rm o} - C_{\rm e}}{C_{\rm e}} \times \frac{V}{m} \tag{3}$$

$$K_{\rm d} = \frac{A_{\rm o} - A_{\rm e}}{A_{\rm e}} \times \frac{V}{m} \tag{4}$$

$$q_{\rm e} = \frac{V(C_{\rm o} - C_{\rm e})}{1000m} \tag{5}$$

$$n_{\rm o} = \frac{C_{\rm o} VR}{1000} \tag{6}$$

$$n_{\rm d} = \frac{C_{\rm o}V - C_{\rm d}V_{\rm d}}{1000} \tag{7}$$

$$D(\%) = \frac{n_{\rm o} - n_{\rm d}}{n_{\rm o}} \times 100\% \tag{8}$$

where m(g) represents the mass of the sorbent. V(mL) refers to the liquid phase volume during the sorption process, V_d (mL) represents the liquid phase volume in the desorption process, $C_{\rm o}$ (µmol L⁻¹) and $C_{\rm e}$ (µmol L⁻¹) denote the starting and final concentrations of metal ions during the sorption process, respectively. C_d (µmol L⁻¹) is the final concentration of metal ions in the desorption process. n_0 (µmol) and n_d (µmol) represent the amount of La³⁺ or Bi³⁺ sorption on the sorbent after the sorption and desorption processes, respectively.

The pseudo-first order (eqn (9)), pseudo-second order (eqn (10)), intraparticle diffusion (eqn (11)) and Elovich (eqn (12)) models were applied to fit sorption kinetic data:38-41

$$q_{t} = q_{e}(1 - e^{-k_{1}t}) \tag{9}$$

$$q_{\rm t} = \frac{k_2 q_{\rm e}^2 t}{1 + k_2 q_{\rm e} t} \tag{10}$$

$$q_{\rm t} = K_{\rm IPD} t^{1/2} + C \tag{11}$$

$$q_{t} = \frac{1}{\beta} \ln(\alpha \beta t + 1) \tag{12}$$

where k_1 (min⁻¹), k_2 (g μ mol⁻¹ min⁻¹), $K_{\rm IPD}$ (μ mol g⁻¹ min^{-1/2}) refer to the sorption rate constants of the kinetic equations. t (min) is the sorption time and $q_{\rm t}$ (μ mol g⁻¹) represents the amount of metal ions adsorbed at time t. C (μ mol g⁻¹) is related to the thickness of boundary layer. α (μ mol g⁻¹ min⁻¹) and β (g μ mol⁻¹) are known as the Elovich coefficients.

The Langmuir and Freundlich models can respectively be expressed as follows eqn (13) and eqn (14), respectively:⁴¹⁻⁴³

$$q_{\rm e} = \frac{K_{\rm L} q_{\rm max} C_{\rm e}}{1 + K_{\rm L} C_{\rm e}} \tag{13}$$

$$q_{\rm e} = K_{\rm F} C_{\rm e}^{\frac{1}{n}} \tag{14}$$

where $K_{\rm L}$ (L µmol⁻¹) is a constant of the Langmuir equation, $q_{\rm max}$ (µmol g⁻¹) represents the maximum amount of metal ions adsorbed onto HDEHP/AC. $K_{\rm F}$ (µmol¹⁻ⁿ Lⁿ g⁻¹) and 1/n are the Freundlich constants related to the sorption capacity and the sorption intensity, respectively.

Results and discussion

3.1. Characterization

HDEHP/AC was characterized by complementary techniques to investigate its physical–chemical properties before testing its performance to separate Bi³⁺ from La³⁺/Ac³⁺. The SEM image revealed irregularly shaped HDEHP/AC grains that ranged from several micrometers to nearly a hundred micrometers in size (Fig. 1a). The XRD pattern (Fig. 1b) exhibited a broad peak centered at around $2\theta=20$ –23°, indicating an amorphous or disordered carbon structures. ^{44,45} Another broad and weak peak was observed at around $2\theta=43$ –44°, which was attributed to an axis of the graphite structure. ^{44,45}

The elemental analysis results (Table S1†) show that the percentage of P in the HDEHP/AC was 2.42 wt%, in addition to 82.8 wt% C, 3.14 wt% H, and 7 wt% O. Furthermore, the DRIFT spectrum (Fig. 1c) of HDEHP/AC contained characteristic bands at 1242 and 1028 cm⁻¹, which were assigned to the P=O and P-O-C stretching modes, respectively.^{46,47} These results indicate that the HDEHP was immobilized onto the activated carbon structure. The introduction of HDEHP on the surface of activated carbons caused a decrease in their specific surface area

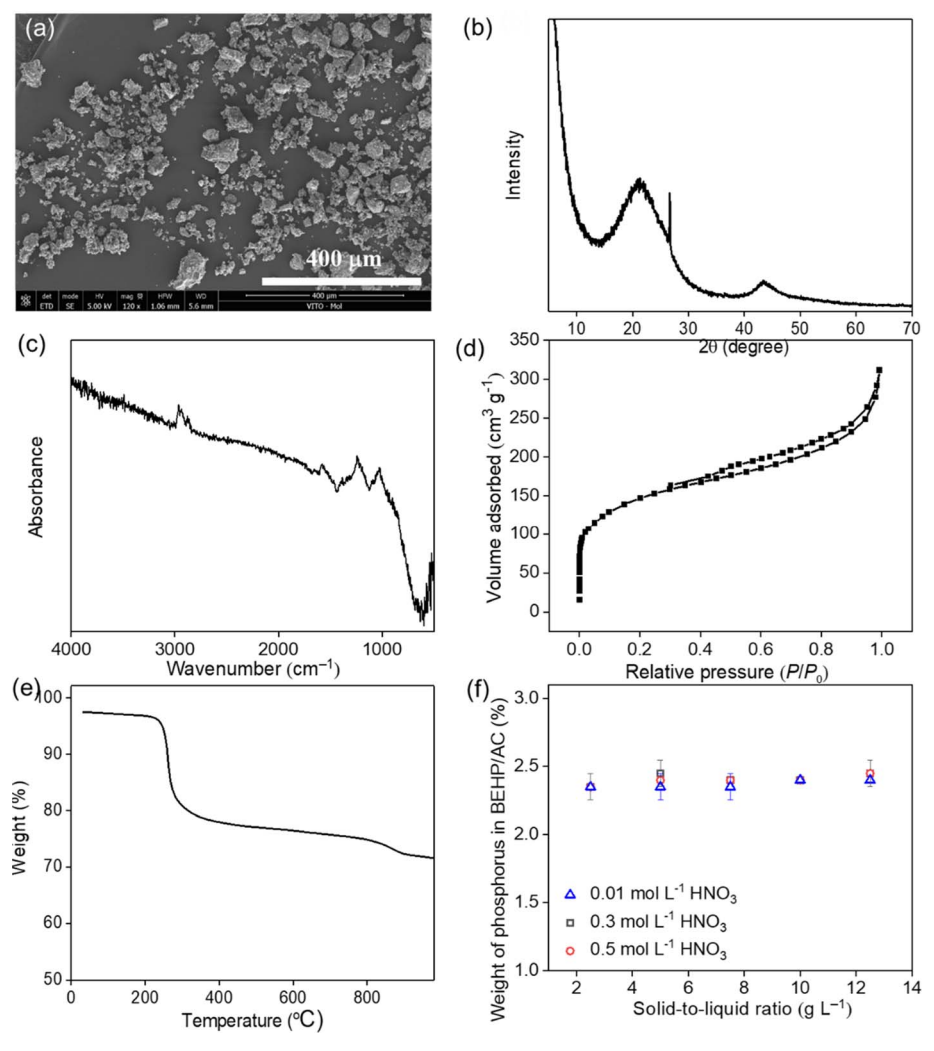


Fig. 1 SEM image (a), XRD pattern (b), FT-IR spectrum (c), N₂ sorption curve (d), TGA curve (e), and phosphorus leaching (f) of HDEHP/AC.

from approximately 1000 m² g⁻¹ (as reported by Merck) to approximately 528 m² g⁻¹, as shown in Table S1† and Fig. 1d. The TGA curve (Fig. 1e) shows that the thermal decomposition of HDEHP/AC began at 230 °C. The mass loss of HDEHP/AC was about 18% up to 400 °C, which was due to the thermal decomposition of HDEHP. Beyond this point, the decomposition rate decreased before reaching \sim 850 °C, indicating that the precursor of activated carbon probably had undergone a carbonization at high temperatures, particularly above 800 °C. Based on above characterization results, there are few other functional groups on the surface of activated carbon, and the primary functional group of HDEHP/AC is the phosphate group. Thus, HDEHP/AC can be used as a sorbent to examine the function of phosphate group and the carbon structure.

For the sorbents, the loss of extractants from the impregnated materials into the liquid phase, due to the dissolution effect and/or mechanical force, was a concern. Therefore, leaching tests have been performed by contacting HDEHP/AC at different solid-to-liquid ratios and in the 0.01–0.5 mol $\rm L^{-1}$ HNO $_3$ solutions for 150 h. Fig. 1f shows phosphorous content in HDEHP/AC after these leaching test, clearly demonstrating that HDEHP is not released from the carbon matrix in such conditions. A further possible reason for this stability was the low solubility of HDEHP in water and the weak HNO $_3$ solutions.

3.2. Sorption performance

3.2.1. Effect of pH. The pH has a significant impact on both the metal speciation and the protonation/deprotonation of the phosphate groups on the HDEHP/AC. 34,50,51 The speciation of La $^{3+}$ and Bi $^{3+}$ as a function of pH was calculated in our previous work. 34 Briefly, La $^{3+}$ and Bi $^{3+}$ ions are present as cations in aqueous solutions when the pH value is below 2.0. Fig. 2a shows the effect of pH on the sorption of La $^{3+}$ /Bi $^{3+}$ onto HDEHP/AC in the binary system (both La $^{3+}$ and Bi $^{3+}$) with a solid-to-liquid ratio of 1 or 2 g L $^{-1}$, respectively.

The La³⁺ sorption percentage and $K_{\rm d}$ values rapidly increased at pH > 1.3. The sorption of La³⁺ onto the HDEHP/AC was primarily due to electrostatic attraction and surface complexation, which is associated with the deprotonated functional groups from HDEHP, known for its p $K_{\rm a}$ of \sim 1.47.⁵² Furthermore, as pH increases, the competitive sorption of decreased H⁺ on HDEHP decrease. Increasing the solid-to-liquid ratio (to 2 g L⁻¹) shifted the increase in sorption capacity to lower pH (by merely 0.2 units), but the overall relationship was not impacted. This reconfirms that the sorption of La³⁺ onto HDEHP/AC was due to the electrostatic attraction/surface complexation and the decreased competitive effect of H⁺. The pH relation also indicates that the La³⁺ is expected to be desorbed *via* ion exchange with H⁺ in relatively low-pH solutions.

In contrast, the Bi^{3+} sorption percentage onto HDEHP/AC increases significantly at a lower pH compared to the increase in sorption capacity for La^{3+} and reaches more than 80% from a pH of 0.9. Increasing the pH further leads to a gradual increase in sorption capacity and related K_{d} values, due to the strong affinity of Bi^{3+} for the sorption active sites. This was probably due to the electrostatic repulsion between Bi^{3+} and

protonated functional groups as well as the competitive sorption of excess H⁺ ions. Increasing the solid-to-liquid ratio leads to a minor shift to higher sorption capacities in the pH range between 0.6 and 1.6.

La³⁺ sorption was also examined over a broad pH range under a single system, as shown in Fig. 2b. The high sorption capacity of HDEHP/AC toward La³⁺ could be achieved at a higher pH value.

Based upon the measured sorption capacity, some estimates can be made for an actual 225 Ac/ 213 Bi generator. In case 4 GBq 225 Ac is loaded onto a column, which corresponds to 8.279 nmol of 225 Ac, only a minor amount of HDEHP/AC as sorbent should be sufficient for full sorption. The pH relationship also offers some insight in the potential use of HDEHP/AC. As selective Bi sorption occurs at low pH (pH < 1), HDEHP/AC could be used in an inverse generator. For a direct generator approach, the pH

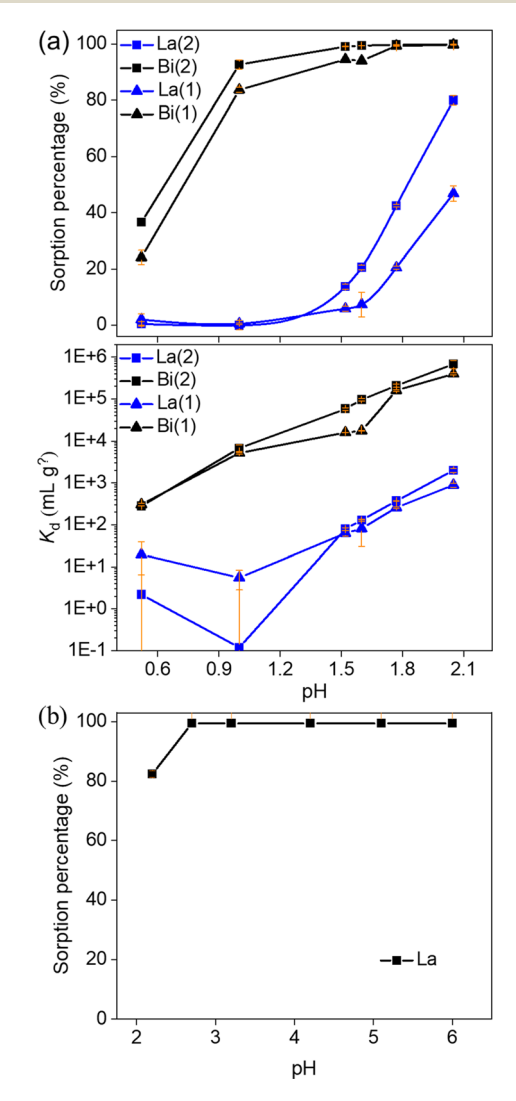


Fig. 2 Effect of pH on the sorption percentage and distribution coefficient (K_d) of HDEHP/AC for La³⁺ and Bi³⁺ in the binary system (a). (C_o (La³⁺) = 10 μ mol L⁻¹ and C_o (Bi³⁺) = 10 μ mol L⁻¹, solid-to-liquid ratio = 1 g L⁻¹ for (1) or 2 g L⁻¹ for (2), t = 24 h). The effect of pH on the sorption percentage of HDEHP/AC for La³⁺ in the single system (b). (C_o (La³⁺) = 10 μ mol L⁻¹, solid-to-liquid ratio = 1 g L⁻¹, t = 24 h).

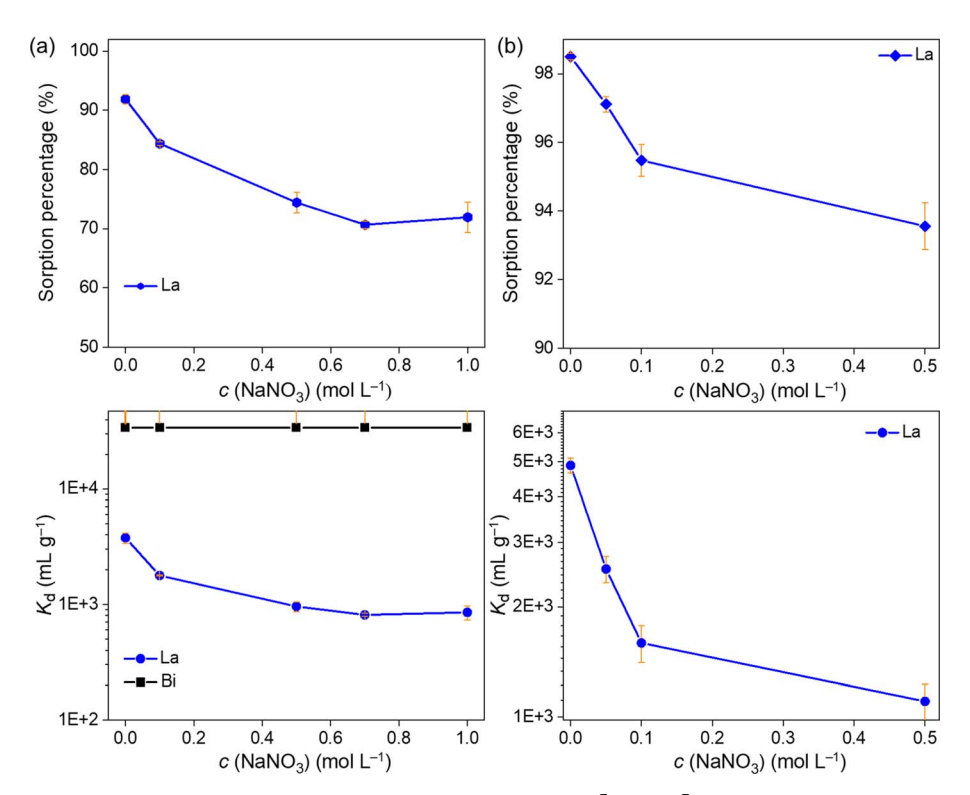


Fig. 3 Effect of NaNO₃ concentration on the sorption performance of HDEHP for La³⁺ and Bi³⁺ in the binary system with a solid-to-liquid ratio of 3 (a) or 13.3 g L⁻¹ (b). (C_o (La³⁺) = 10 μ mol L⁻¹ and C_o (Bi³⁺) = 10 μ mol L⁻¹, pH = 2, t = 24 h).

and the solid-to-liquid ratio can be increased to facilitate the sorption of both Bi^{3+} and La^{3+} .

According to above results, we inferred that controlling the separation pH (*e.g.*, pH = 0.6) is expected to facilitate the selective uptake of Bi³⁺ from a La³⁺(Ac³⁺)/Bi³⁺ mixed solution onto the inverse separation column filled with HDEHP/AC sorbent. The use of sorbents with phosphate functional groups in the inverse generators is expected to align with our previous research.³⁴ For the direct separation column, when the pH > 2 or 3, a high sorption capacity for La³⁺ (Ac³⁺) onto HDEHP/AC is expected to be achieved by increasing the pH and solid-to-liquid ratio.

3.2.2. Effect of NaNO₃ concentration. Fig. 3a presents impact of ionic strength on the separation of La3+/Bi3+ by varying the NaNO₃ concentrations. The removal percentages and K_d values for La³⁺ gradually decreased as the concentration of NaNO₃ increased from 0 to 1.0 mol L⁻¹, attributed to the shrinkage of the electrical double layer and thus a weaker electrostatic attraction between La3+ and HDEHP/AC.53 The increased influence of ion competition with higher concentrations of interfering ions in the solution reduced the availability of La³⁺ ions for sorption. By contrast, the K_d values for the Bi³⁺ remained very high throughout the concentration range and appeared to be independent of the NaNO3 concentration, indicating that a different sorption mechanism is at play for Bi³⁺. Additionally, the La³⁺ sorption percentage increased as the solid-to-liquid ratio increased from 3 to 13.3 g L^{-1} (Fig. 3b). The sorption percentages and K_d values for La³⁺ were still greater than 90% and 10³ mL g⁻¹, respectively, when the NaNO₃

solution was below 0.5 mol L^{-1} at pH = 2 with a solid-to-liquid ratio of 13.3 g L^{-1} . This suggests that the negative effect of ionic strength could be attenuated by increasing the solid-to-liquid ratio.

3.2.3. Effect of halide ion concentration. The influence of halide ions on the sorption performance of HDEHP/AC toward La^{3+}/Bi^{3+} was examined using 0.1–1.0 mol L^{-1} NaCl and 0.1–0.5 mol L^{-1} NaI solutions. Fig. 4a shows that the Bi^{3+} sorption percentages decreased significantly as the NaCl concentration increased at pH = 2 and pH = 0.5, due to the formation of Bi–Cl complexes (*e.g.*, $[BiCl_4]^-$), which have a lower affinity for HDEHP/AC.⁵⁴ This effect of decreasing sorption capacity is more pronounced at lower pH values, indicating that the H^+ concentration was also an influencing factor. The La^{3+} sorption percentage at pH = 2 gradually decreased as the NaCl concentration increase, due to the influence of ionic strength, but remains higher than 80% even in the presence of 1 mol L^{-1} NaCl.

Also these results indicate the potential in a generator, in which ${\rm Bi}^{3^+}$ can be selectively eluted from the column at a relatively high pH (e.g., pH = 2), with minimal effect on the La³⁺ sorption. One possible reason for this phenomenon was the electrostatic repulsion that likely occurred between the negatively charged Bi-anion complexes and the deprotonated functional groups, which were also negatively charged.^{54,55} Furthermore, lowering the pH could elute the high Bi³⁺ in a relatively low concentration of NaCl, but this process also resulted in the elution of most of the La³⁺ from HDEHP/AC.

Paper RSC Advances

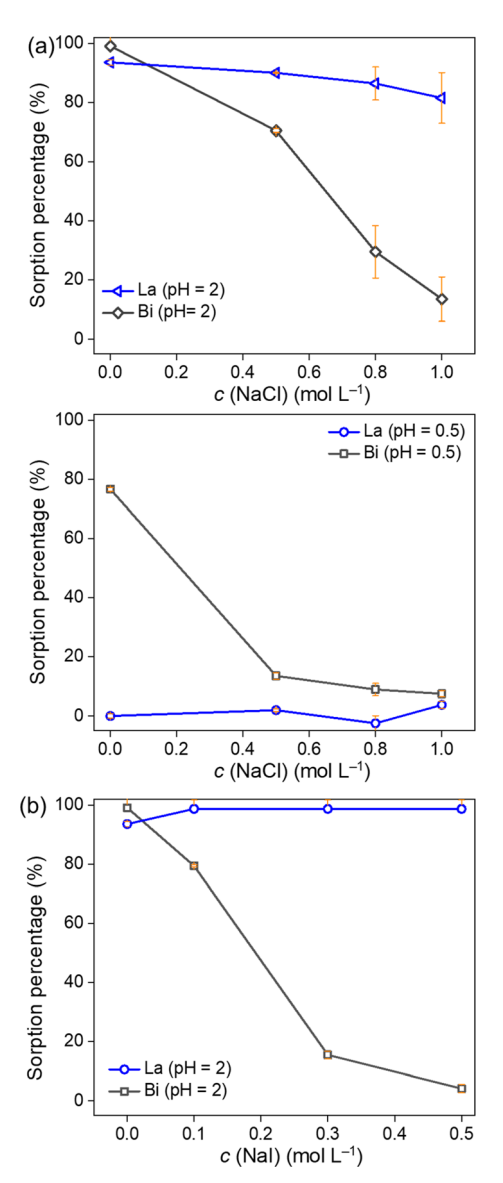


Fig. 4 Effect of NaCl (a) and Nal (b) concentration on the sorption performance of HDEHP for La $^{3+}$ and Bi $^{3+}$ in the binary system. ($C_{\rm o}$ (La $^{3+})=10~\mu{\rm mol}~{\rm L}^{-1}$ and $C_{\rm o}$ (Bi $^{3+})=10~\mu{\rm mol}~{\rm L}^{-1}$, solid-to-liquid ratio $=13.3~{\rm g}~{\rm L}^{-1},~t=24~{\rm h}).$

The profound effect of chloride ions on the sorption performance is also noticed for iodide. Fig. 4b shows the very high La³+ sorption capacity (>98%) in the presence of NaI concentrations in the range of 0.1 to 0.5 mol L $^{-1}$ (at pH = 2). Similar to NaCl, increasing the NaI concentration drastically decreases the Bi³+ sorption capacity, due to the formation of Biiodide complexes which seem to have an even lower affinity compared to the Bi-chloride complexes. In summary, the halide ions (e.g., Cl $^-$ and I $^-$) are expected to selectively elute 213 Bi from the direct 225 Ac/ 213 Bi columns, resulting in the electrostatic repulsion between the Bi-halide anions and the negatively charged phosphate groups. 54,55

3.2.4. Effect of sorption time. The sorption kinetics of La³⁺ and Bi³⁺ onto the HDEHP/AC were determined by sorption experiments at time intervals in the range of 2–180 min. Fig. 5a

presents of the evolution of the La³⁺/Bi³⁺ sorption percentages as a function of the contact time for single and binary systems. The sorption of La³⁺/Bi³⁺ onto HDEHP/AC rapidly increased within the first period (<30 min), which was attributed to the availability of sufficient active sites for La³⁺/Bi³⁺ sorption. Then, sorption slightly increased because of the depletion of Bi³⁺ from the solution and the limited accessible active sites for La³⁺. Additionally, the Bi³⁺ sorption capacity was noticeably higher compared to the La³⁺ sorption capacity.

The sorption of La³⁺ was distinctly higher in the single system than in the binary system at the corresponding time points, indicating that the presence of Bi³⁺ had a significant effect on the La³⁺ sorption. This was because most of the sorption sites were occupied by Bi³⁺. However, in practical applications, the concentration of Bi³⁺ is expected to be much lower than that of La³⁺ due to the high specific activity of ²¹³Bi³⁺ compared to ²²⁵Ac³⁺. As such, the negative impact of Bi³⁺ on the La³⁺ sorption percentage would be less pronounced, as seen in Fig. 5a. By contrast, the Bi³⁺ sorption was not influenced by the presence of La³⁺, which was attributed to the high affinity of HDEHP/AC for Bi³⁺ as well as the fast kinetic interaction times.

Pseudo-first-order, pseudo-second-order, intraparticle diffusion and Elovich sorption kinetic models were applied to fit the experimental data and to obtain insight into the underlying sorption mechanism.³⁹⁻⁴¹ The fitting parameters are shown in Table S2.† In the single system (Fig. 5b), the pseudo-secondorder equation had high correlation coefficient values that indicated its suitability for illustrating the sorption process of La³⁺ and Bi³⁺ onto the HDEHP/AC. A similar result was obtained in the binary system (Fig. 5c). Based on the pseudo-secondorder equation, the q_e (La³⁺) in the single system (5.590 μ mol g^{-1}) was higher than that in the binary system (4.069 μ mol g^{-1}), suggesting that competitive sorption occurred. There were no obvious changes in Bi3+ sorption, indicating the weak competition of La³⁺ for Bi³⁺. Furthermore, compared to the pseudofirst-order and pseudo-second-order models, the intraparticle diffusion model was not suitable for the kinetic results due to its low R^2 value (Fig. 5d). Interestingly, the Elovich model provided a better fit the kinetic data of La³⁺ among the four models (Fig. 5d). Based on these comparisons, it can be concluded that the kinetic behavior for La³⁺ can be described by the Elovich model, while the pseudo-second-order is more appropriate for Bi³⁺.

3.2.5. Effect of initial La³⁺/**Bi**³⁺ **concentration.** The influence of starting La³⁺ and Bi³⁺ concentration on the sorption performance was also studied in the single/binary systems, and the relevant results are presented in Fig. 6a. The La³⁺ sorption onto HDEHP/AC increased rapidly as the initial concentration of La³⁺ increased and then increased slightly, which was ascribed to the saturation of active sorption sites. The sorption capacity of HDEHP/AC for La³⁺ was higher in the single system than in the binary system, attributed to the faster kinetics of the Bi³⁺ sorption leading to an occupation of the available sorption sites (competitive sorption of Bi³⁺ over La³⁺). Additionally, the sorption capacity and sorption percentages for Bi³⁺ were still very high across the entire range. Fig. 6b illustrates that the La³⁺ sorption percentages of HDEHP/AC decreased linearly with

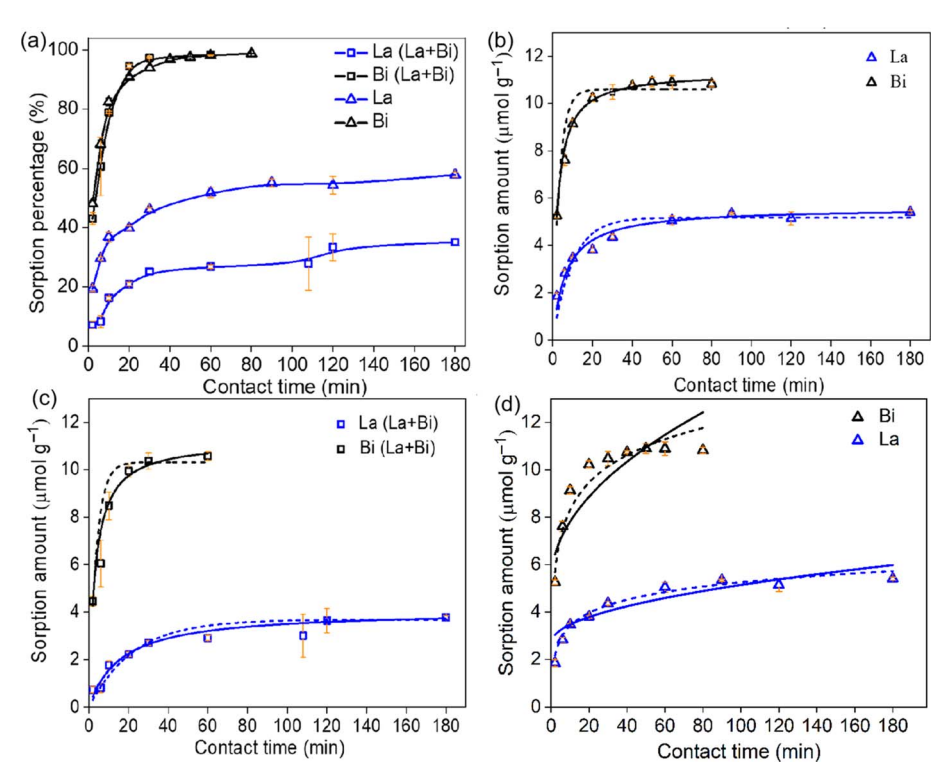


Fig. 5 Effect of contact time on the sorption performance of HDEHP/AC for La^{3+}/Bi^{3+} in the single (La/Bi) and binary (La + Bi) systems (a). Sorption kinetics of La^{3+} or Bi^{3+} onto HDEHP/AC in the single (b) and binary (c) systems (pseudo-first-order curve: dashed line, pseudo-second-order curve: solid line). Sorption kinetics of La^{3+} or Bi^{3+} onto HDEHP/AC in the single system (d) (intraparticle diffusion model: solid line, Elovich model: dashed line). (C_o (La^{3+}) = 10 μ mol L^{-1} and/or C_o (Bi^{3+}) = 10 μ mol L^{-1} , solid-to-liquid ratio = 1 g L^{-1} , μ pH = 2).

increasing La3+ and Bi3+ concentrations. However, this is unlikely to significantly affect ²²⁵Ac/²¹³Bi separation in a direct generator as the loading amount of ²²⁵Ac in practical applications is low. Moreover, this finding suggests a useful strategy for the inverse generator, where La3+ absorbed on the column prior to loading ²²⁵Ac and ²¹³Bi solution is expected to reduce the ²²⁵Ac sorption. The La³⁺ in the ²¹³Bi eluate can then be purified using a guard column (e.g., AG MP-50 column). The Langmuir and Freundlich models were used to fit the La3+ data in the single system, with the curves shown in Fig. 6c and the relevant parameters presented in Table S3.†41-43 The Langmuir model was more suitable to describe the La³⁺ sorption process than the Freundlich model according to the R^2 . This indicates that all of the active sites for La³⁺ had equal adsorption affinities and were energetically and sterically independent of the adsorbed quantity. 41,56 The maximum La3+ sorption capacity of HDEHP/AC was 15.226 μ mol g⁻¹.

3.2.6. Effect of gamma-ray irradiation. The radiation stability of HDEHP/AC is also an important influencing factor that affects its performance as a sorbent material. In this study, HDEHP/AC was exposed to 862 ± 121 kGy under dry conditions to investigate its radiation stability. Fig. 7a and b shows the $K_{\rm d}$ values and sorption percentages upon the HDEHP/AC exposure to 0 and 862 kGy, respectively. The La³⁺ sorption percentage decreased, which was probably due to the cleavage of the C–C bond and the scission of the C–PO₄ bond of the HDEHP/AC after exposure to gamma-radiation (Fig. 7c) as also illustrated

in the previous studies^{23,26} However, there was no noticeable change in the sorption capacity of HDEHP/AC for Bi3+, due to the presence of sufficient sorption sites for Bi³⁺. Based on these findings, one potential approach to enhance the operation time of the generator would be to introduce a low density of phosphate groups into the carbon structure. This modification is expected to decrease radiation damage to sorbents when loaded with high-activity radioisotopes. The relatively fewer number of active sites may not pose a significant problem for ²²⁵Ac/²¹³Bi generator columns, due to the low amount of ²²⁵Ac and ²¹³Bi isotopes in practical applications. Another potential approach would involve reducing radiation damage and prolonging the lifetime of the generator, to minimize the contact time between the sorbents and ²²⁵Ac and its daughter nuclides. This could be achieved by eluting ²²⁵Ac from the column, as described in the following section.

3.2.7. ²²⁵Ac sorption behavior on HDEHP/AC. La³⁺ was used as a surrogate of Ac³⁺ due to similar sorption changes with varying HNO₃ concentrations, as reported in previous studies on the La³⁺ and Ac³⁺ sorption.²⁷ The similar sorption behaviors were possibly due to their stable valence charge (+3) in aqueous solution, hydrolysis properties, and absolute chemical hardness (15.4 eV for La³⁺, whereas 14.4 eV for Ac³⁺).⁵⁷⁻⁵⁹ However, it should be noted that the phosphate groups had a stronger sorption affinity toward La³⁺ than Ac³⁺. Herein, the sorption capacity of HDEHP/AC toward ²²⁵Ac³⁺ was also investigated by conducting batch sorption experiments, providing the reference

Paper

(a) 16 Sorption amount (µmol g⁻¹) 14 12 10 8 6 Bi (La+Bi) 4 La (La+Bi) 2 30 45 60 Initial concentration (µmol L-1) (b)₁₀₀ Sorption percentage (%) 80 60 40 Bi (La+Bi) 20 La (La+Bi) La 0 45 15 30 60 Initial concentration (µmol L-1) (c) 16 Sorption amount (µmol g⁻¹) 14 12 10 8 6 4 2

Fig. 6 Effect of initial concentration for La³⁺/Bi³⁺ sorption onto HDEHP/AC in the single (La/Bi) and binary (La + Bi) systems (a and b). Sorption isotherms of La³⁺ onto HDEHP/AC in the single system (Langmuir isotherm: solid line, Freundlich isotherms: dashed line) (c). (Solid-to-liquid ratio = 2 g L^{-1} , pH = 2, t = 24 h).

5 10 15 20 25 Equilibrium concentration (μmol L⁻¹)

sorption performance of ²²⁵Ac³⁺ on HDEHP/AC. Fig. 8 presents the increase in Ac3+ sorption percentage as pH increases, whereas the sorption capacity could also be improved with the increased solid-to-liquid ratio. Although the sorption capacity of Ac³⁺ onto these types of materials with phosphate groups was lower than that of La³⁺ sorption (see Fig. 2a), both exhibited similar sorption behaviors. Therefore, investigating La³⁺ sorption could still provide reliable guidance for Ac3+ sorption onto HDEHP/AC.

3.3. Desorption performance

The recycling of ²²⁵Ac is also an essential step for the generator column, as most functional groups are susceptible to radiolytic damage. Additionally, in the direct system, reducing the contact

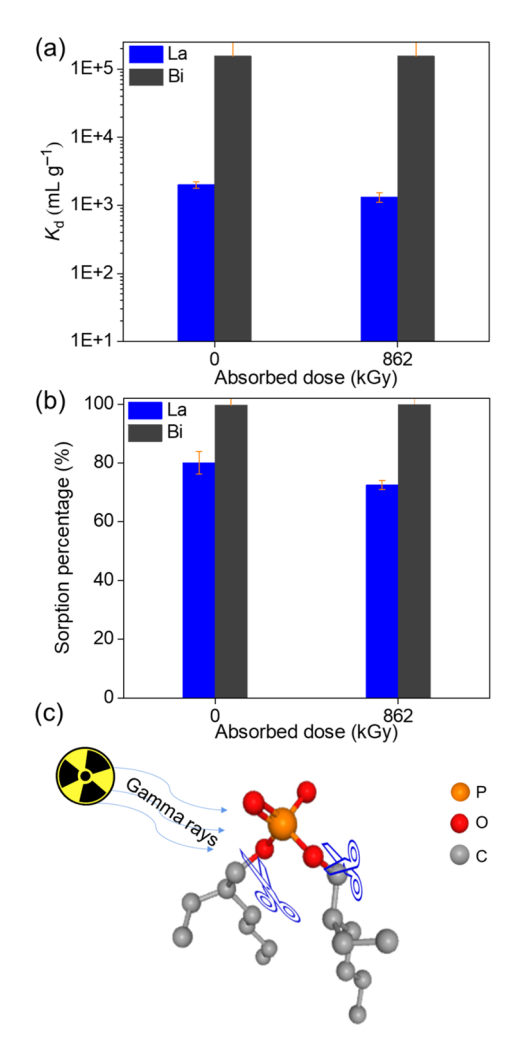


Fig. 7 Effect of absorbed dose on the distribution coefficient (a) and sorption percentage (K_d) (b) of HDEHP/AC for La³⁺ and Bi³⁺ in the binary system. (C_o (La³⁺) = 10 μ mol L⁻¹ and C_o (Bi³⁺) = 10 μ mol L⁻¹ solid-to-liquid ratio = 2 g L⁻¹, pH = 2, t = 24 h). Schematic illustration of scission of functional groups by gamma irradiation (c).

time is an effective way to minimize the dose received by the sorbents. This study investigated the effectiveness of the HNO₃ solution in desorbing La³⁺ from the HDEHP/AC. Fig. 9a shows that 0.1 mol L⁻¹ HNO₃ solution could desorb nearly 90% of the La³⁺, while almost all of the La³⁺ on HDEHP/AC could be desorbed using 0.2–0.3 mol L^{-1} HNO $_3$ solution. Considering the influence of ionic strength, ²²⁵Ac could be readily reused with a salt concentration of less than 0.5 mol L⁻¹. An interesting finding was the relatively low desorption capacity of Bi³⁺, suggesting the potential use of HNO3 for the selective desorption of ²²⁵Ac in the inverse generator. This step could improve the purity of ²¹³Bi without significantly affecting its yield. Fig. 9b shows the desorption of Bi^{3+} from HDEHP/AC at pH = 2, using NaI solution. The results show that the desorption percentage of Bi³⁺ increased with the NaI concentration increasing, while there was no desorption efficiency for La³⁺. This indicates that the Bi³⁺ could be selectively desorbed.

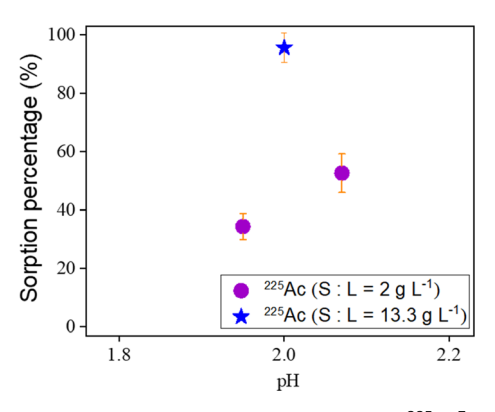


Fig. 8 Sorption percentage of HDEHP/AC towards $^{225}\text{Ac}^{3+}$. (Ao = 100 kBq, Co (La $^{3+}$) = 10 $\mu mol~L^{-1}$ and Co (Bi $^{3+}$) = 10 $\mu mol~L^{-1}$, t = 2 h).

3.4. Preliminary column test

To evaluate the 225 Ac/ 213 Bi separation performance for practical applications, a column test is needed. However, commercial HDEHP/AC consisted of an irregular powder with a broad particle size range, making it difficult to increase the flow rate of the solution due to the high-pressure stacking. Nevertheless, a preliminary column test was conducted to offer some guidance for further material design. The 213 Bi yield was approximately 50% in the 5 mL of 1 mol L $^{-1}$ NaI/0.01 mol L $^{-1}$ HNO $_{3}$

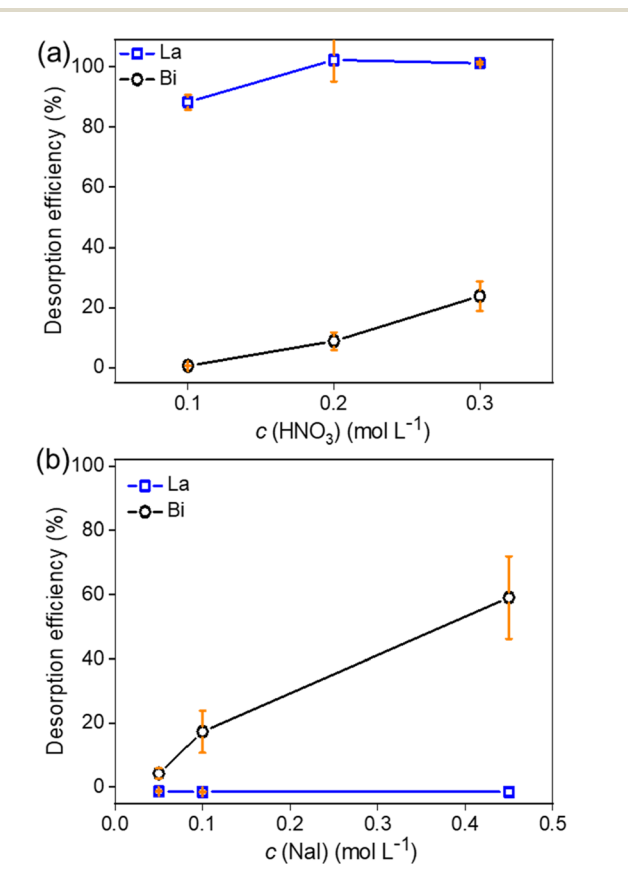


Fig. 9 The desorption efficiency of La^{3+} and Bi^{3+} from the HDEHP/AC as of function of HNO_3 (a) concentration and Nal concentration (pH = 2) (b).

eluate, with the ²²⁵Ac impurity being less than 0.04%. The ²¹³Bi yield was lower compared to previously used materials, due to the high surface areas of the carbon structures. Additionally, a high mass value of HDEHP/AC was used during the desorption process, resulting in low desorption efficiency. However, this result also indicates that the grafting of phosphate functional groups onto the carbon materials could serve as a potential candidate for use in the direct ²²⁵Ac/²¹³Bi generators.

3.5. Conceptual separation of ²²⁵Ac and ²¹³Bi

The findings of this study suggest that the phosphate groups and carbon structure had the potential to serve as the active sites and support, respectively, for the ²¹³Bi separation. Although commercial HDEHP/AC was unsuitable for practical use, the data obtained could serve as a reference for designing materials and optimizing separation processes. Shaped HDEHP/AC materials with a suitable range of particle sizes could be fabricated and utilized for ²²⁵Ac/²¹³Bi separation. The conceptual separation of ²²⁵Ac and ²¹³Bi based upon this material can be envisioned in several approaches.

The first approach is a 2-column direct generator, as shown in Fig. 10a. The detailed separation process can be seen in the experimental section. The second column can be used for the further purification of ²¹³Bi eluate. An alternative use in a direct generator, consists in the removal of two-thirds of the sorbent

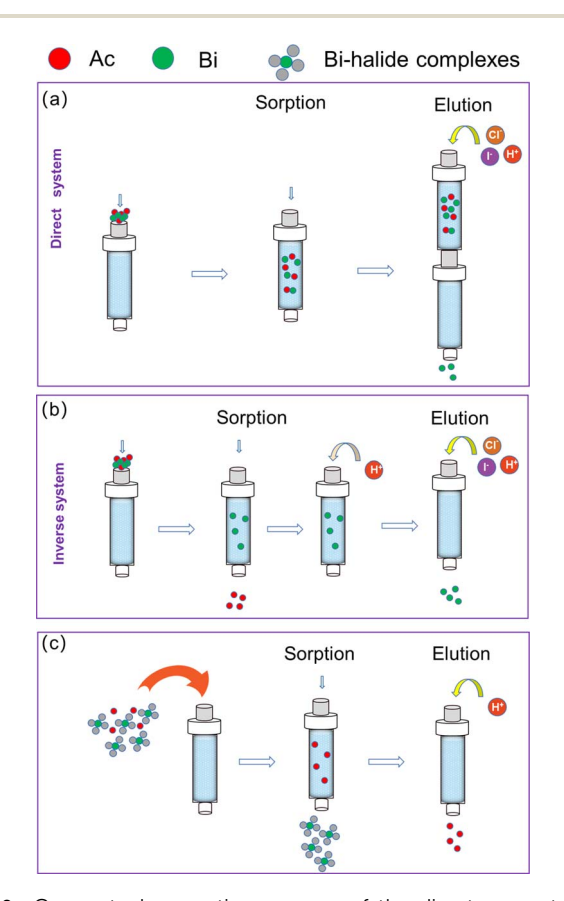


Fig. 10 Conceptual separation process of the direct generator (a), inverse generator (b), and a possible method (c).

from the column for adsorbing ²²⁵Ac and ²¹³Bi through batch experiments, and then the sorbents with 225Ac/213Bi can be placed back into the column.29 A guard column with AG MP-50 or its analog could also be employed to improve the purity of ²¹³Bi. Before the sorbents experienced severe damage, the ²²⁵Ac could be readily eluted from HDEHP/AC using relatively weak acidic solutions compared to the AG MP-50.

The material holds also potential to be used in an inverse generator (see Fig. 10b). Bi3+ could be selectively adsorbed onto HDEHP/AC by adjusting the pH and salt concentrations. The purity of Bi3+ could be further improved by using 0.1-0.2 mol L⁻¹ HNO₃ to elute the possibly adsorbed ²²⁵Ac³⁺ before the ²¹³Bi eluting step. This method could significantly reduce the radiolytic damage for the sorbents. Additionally, this separation is similar to the PNNL Bi-generator concept.11

HDEHP/AC also showed selective sorption of ²²⁵Ac, with minimal sorption capacity for Bi-halide complexes, as shown in Fig. 10c. When the ²²⁵Ac and ²¹³Bi-halide complexes pass through the column, the ²²⁵Ac can be selectively adsorbed onto the column. The ²¹³Bi can be obtained in a vial. Subsequently, the ²²⁵Ac can be eluted from the column for ²¹³Bi ingrowth for use in the next cycle.

Conclusions

The study investigated the sorption and desorption behaviors of La³⁺ (as an analog for ²²⁵Ac) and Bi³⁺ by HDEHP/AC for the selective separation of ²¹³Bi in medical applications. HDEHP/ AC exhibited sorption toward La3+ via electrostatic attraction and surface complexation with a maximum sorption capacity of about 15 μ mol g⁻¹ (from the Langmuir model) at pH = 2, which could be further increased by increasing the pH values. The sorption of La3+ onto HDEHP/AC could be fitted by the Elvoich model. Further research shows that the La³⁺ sorption capacity decreased slightly or did not change as the NaCl and NaI concentrations increased, in contrast with the Bi³⁺ sorption capacity which decreased rapidly for Bi3+ owing to the formation of Bi-halide complexes. The desorption results show that the La³⁺ could be completely eluted from the sorbent via 0.2-0.3 mol L⁻¹ HNO₃ solutions from HDEHP/AC, which was likely to be beneficial in reducing the radiation damage to the direct column and for recycling undecayed ²²⁵Ac. Additionally, Bi³⁺ could be selectively adsorbed by HDEHP/AC at a low pH and relatively high NaNO3 concentration, and the HNO3 could be used to further improve the ²¹³Bi purity in the inverse generator. Simultaneously, large amounts of Bi³⁺ are expected to be eluted by halide ions at a low pH (e.g., pH = 0.5) from the inverse columns. Therefore, HDEHP/AC showed promise for application in direct and inverse ²²⁵Ac/²¹³Bi generators. However, commercial HDEHP/AC is an irregular powder with a broad particle size range and a high specific surface area, limiting its application in column chromatography. Further research should be dedicated towards the development if synthesis routes to graft phosphate groups onto shaped carbon materials (or alternatives) and to optimize the separation process conditions.

Data availability

The data supporting this article have been included as part of the ESI.†

Conflicts of interest

The authors declare that they have no known competing financial interests or personal relationships that could have appeared to influence the work reported in this paper.

Acknowledgements

The SCK CEN and VITO are acknowledged for funding. Furthermore, the authors would like to acknowledge the technical assistance of P. Verheyen (ICP-MS), K. Raymond (SEM), K. Zhang & V. Meynen (DRIFT), M. Mertens (XRD), A. De Wilde (N2 sorption and TGA-MS), and J. De Wit (CHN analysis).

References

- 1 G. Sgouros, L. Bodei, M. R. McDevitt and J. R. Nedrow, Radiopharmaceutical therapy in cancer: clinical advances and challenges, Nat. Rev. Drug Discov., 2020, 19, 589-608.
- 2 Targeted Alpha Therapy Working Group, C. Parker, V. Lewington, N. Shore, C. Kratochwil, M. Levy, O. Linden, W. Noordzij, J. Park and F. Saad, Targeted Alpha Therapy, an Emerging Class of Cancer Agents: A Review, JAMA Oncol., 2018, 4, 1765-1772.
- 3 H. Zhu, S. Heinitz, K. Binnemans, S. Mullens and T. Cardinaels, ²²⁵Ac/²¹³Bi radionuclide generators for the separation of ²¹³Bi towards clinical demands, *Inorg. Chem.* Front., 2024, 11, 4499-4527.
- 4 A. Morgenstern, C. Apostolidis, C. Kratochwil, M. Sathekge, L. Krolicki and F. Bruchertseifer, An Overview of Targeted Alpha Therapy with 225 Actinium and 213 Bismuth, Curr. Rad., 2018, 11, 200-208.
- 5 A. K. H. Robertson, C. F. Ramogida, P. Schaffer and ²²⁵Ac Radchenko, V. Development of TRIUMF Radiopharmaceuticals: Perspectives and Experiences, Curr. Rad., 2018, 11, 156-172.
- 6 S. Ahenkorah, I. Cassells, C. M. Deroose, T. Cardinaels, A. R. Burgoyne, G. Bormans, M. Ooms and F. Cleeren, Bismuth-213 for Targeted Radionuclide Therapy: From Atom to Bedside, Pharmaceutics, 2021, 13, 599.
- 7 C. Kratochwil, F. L. Giesel, F. Bruchertseifer, W. Mier, C. Apostolidis, R. Boll, K. Murphy, U. Haberkorn and A. Morgenstern, ²¹³Bi-DOTATOC receptor-targeted alpharadionuclide therapy induces remission in neuroendocrine tumours refractory to beta radiation: a first-in-human experience, Eur. J. Nucl. Med. Mol. Imag., 2014, 41, 2106-2119.
- 8 S. Ermolaev, A. Skasyrskaya and A. Vasiliev, A Radionuclide Generator of High-Purity Bi-213 for Instant Labeling, Pharmaceutics, 2021, 13, 914.

- 9 A. N. Vasiliev, V. A. Zobnin, Y. S. Pavlov and V. M. Chudakov, Radiation Stability of Sorbents in Medical ²²⁵Ac/²¹³Bi Generators, *Solvent Extr. Ion Exch.*, 2020, **39**, 353–372.
- 10 M. R. McDevitt, R. D. Finn, G. Sgouros, D. Ma and D. A. Scheinberg, An ²²⁵Ac/²¹³Bi generator system for therapeutic clinical applications: construction and operation, *Appl. Radiat. Isot.*, 1999, **50**, 895–904.
- 11 L. A. Bray, J. M. Tingey, J. R. DesChane, O. B. Egorov, T. S. Tenforde, D. S. Wilbur, D. K. Hamlin and P. M. Pathare, Development of a Unique Bismuth (Bi-213) Automated Generator for Use in Cancer Therapy, *Ind. Eng. Chem. Res.*, 2000, 39, 3189–3194.
- 12 V. Beaugeard, J. Muller, A. Graillot, X. Ding, J.-J. Robin and S. Monge, Acidic polymeric sorbents for the removal of metallic pollution in water: A review, *React. Funct. Polym.*, 2020, 152, 104599.
- 13 M. W. Geerlings, F. M. Kaspersen, C. Apostolidis and R. V. Der Hout, The feasibility of 225 Ac as a source of α -particles in radioimmunotherapy, *Nucl. Med. Commun.*, 1993, **14**, 121–125.
- 14 A. Morgenstern, F. Bruchertseifer and C. Apostolidis, Bismuth-213 and Actinium-225 – Generator Performance and Evolving Therapeutic Applications of Two Generator-Derived Alpha-Emitting Radioisotopes, *Curr. Rad.*, 2012, 5, 221–227.
- 15 H. Zhu, S. Heinitz, S. Eyley, W. Thielemans, E. Derveaux, P. Adriaensens, K. Binnemans, S. Mullens and T. Cardinaels, Gamma radiation effects on AG MP-50 cation exchange resin and sulfonated activated carbon for bismuth-213 separation, *RSC Adv.*, 2023, 13, 30990–31001.
- 16 C. Apostolidis, B. Brandalise, R. Carlos-Marquez, W. Janssens, R. Molinet and T. Nikula, Method of loading a radioelement generator with mother radionuclide, *US Pat.*, US2005/0008553, 2005.
- 17 L. M. Arrigo, J. Jiang, Z. S. Finch, J. M. Bowen, C. L. Beck, J. I. Friese, L. R. Greenwood and B. N. Seiner, Development of a separation method for rare earth elements using LN resin, J. Radioanal. Nucl. Chem., 2020, 327, 457–463.
- 18 C. D. Smith and M. L. Dietz, Support loading effects on the performance of an extraction chromatographic resin: Toward improved separation of trivalent lanthanides, *Talanta*, 2021, 222, 121541.
- 19 X. Huang, J. Dong, L. Wang, Z. Feng, Q. Xue and X. Meng, Selective recovery of rare earth elements from ion-adsorption rare earth element ores by stepwise extraction with HEH(EHP) and HDEHP, *Green Chem.*, 2017, 19, 1345–1352.
- 20 S. S. Kumar, A. Rao, K. K. Yadav, R. K. Lenka, D. K. Singh and B. S. Tomar, Selective removal of Am(III) and Pu(IV) from analytical waste solutions of quality control operations using extractant encapsulated polymeric beads, *J. Radioanal. Nucl. Chem.*, 2020, 324, 375–384.
- 21 E. P. Horwitz, R. Chiarizia and M. L. Dietz, DIPEX: A new extraction chromatographic material for the separation and preconcentration of actinides from aqueous solution, *React. Funct. Polym.*, 1997, 33, 25–36.

- 22 W. Wang and C. Y. Cheng, Separation and purification of scandium by solvent extraction and related technologies: a review, *J. Chem. Technol. Biotechnol.*, 2011, **86**, 1237–1246.
- 23 K. K. S. Pillay, A review of the radiation stability of ion exchange materials, *J. Radioanal. Nucl. Chem.*, 1986, **102**, 247–268.
- 24 M. Chen, Z. Li, Y. Geng, H. Zhao, S. He, Q. Li and L. Zhang, Adsorption behavior of thorium on N,N,N',N'-tetraoctyldiglycolamide (TODGA) impregnated graphene aerogel, *Talanta*, 2018, **181**, 311–317.
- 25 T. Kawamura, H. Wu and S.-Y. Kim, Adsorption and separation behavior of strontium and yttrium using a silica-based bis(2-ethylhexyl) hydrogen phosphate adsorbent, J. Radioanal. Nucl. Chem., 2021, 329, 1001–1009.
- 26 Q. Shu, A. Khayambashi, X. Wang, X. Wang, L. Feng and Y. Wei, Effects of γ irradiation on bis(2-ethylhexyl) phosphoric acid supported by macroporous silica-based polymeric resins, *Radiochim. Acta*, 2018, **106**, 249–258.
- 27 V. Ostapenko, A. Vasiliev, E. Lapshina, S. Ermolaev, R. Aliev, Y. Totskiy, B. Zhuikov and S. Kalmykov, Extraction chromatographic behavior of actinium and REE on DGA, Ln and TRU resins in nitric acid solutions, *J. Radioanal. Nucl. Chem.*, 2015, 306, 707-711.
- 28 N.-E. Belkhouche and N. Benyahia, Modeling of Adsorption of Bi(III) from Nitrate Medium by Impregnated Resin D₂EHPA/XAD-1180, *J. Surf. Eng. Mater. Adv. Technol.*, 2011, **01**, 30–34.
- 29 C. Wu, M. W. Brechbiel and O. A. Gansow, An Improved Generator for the Production of ²¹³Bi from ²²⁵Ac, *Radiochim. Acta*, 1997, **79**, 141–144.
- 30 W. Yantasee, G. E. Fryxell, K. Pattamakomsan, T. Sangvanich, R. J. Wiacek, B. Busche, R. S. Addleman, C. Timchalk, W. Ngamcherdtrakul and N. Siriwon, Selective capture of radionuclides (U, Pu, Th, Am and Co) using functional nanoporous sorbents, *J. Hazard. Mater.*, 2019, 366, 677–683.
- 31 W. A. Abbasi and M. Streat, Sorption of uranium from nitric acid solution using TBP-impregnated activated carbons, *Solvent Extr. Ion Exch.*, 1998, **16**, 1303–1320.
- 32 E. P. Horwitz and C. A. A. Bloomquist, Chemical separations for super-heavy element searches in irradiated uranium targets, *J. Inorg. Nucl. Chem.*, 1975, 37, 425–434.
- 33 L. Ondrák, K. Ondrák Fialová, M. Sakmár, M. Vlk, F. Bruchertseifer, A. Morgenstern and J. Kozempel, Development of ²²⁵Ac/²¹³Bi generator based on α-ZrP-PAN composite for targeted alpha therapy, *Nucl. Med. Biol.*, 2024, 132–133, 108909.
- 34 H. Zhu, S. Heinitz, S. Eyley, W. Thielemans, K. Binnemans, S. Mullens and T. Cardinaels, Sorption and desorption performance of La³⁺/Bi³⁺ by surface-modified activated carbon for potential application in medical ²²⁵Ac/²¹³Bi generators, *Chem. Eng. J.*, 2023, **464**, 142456.
- 35 F. Monroy-Guzman, C. d. C. De la Cruz Barba, E. Jaime Salinas, V. Garibay-Feblés and T. N. Nava Entzana, Extraction Chromatography Materials Prepared with HDEHP on Different Inorganic Supports for the Separation of Gadolinium and Terbium, *Metals*, 2020, **10**, 1390.

Paper

36 E. A. El-Sofany, W. F. Zaher and H. F. Aly, Sorption potential of impregnated charcoal for removal of heavy metals from phosphoric acid, *J. Hazard. Mater.*, 2009, **165**, 623–629.

- 37 Z. Heidarinejad, M. H. Dehghani, M. Heidari, G. Javedan, I. Ali and M. Sillanpää, Methods for preparation and activation of activated carbon: a review, *Environ. Chem. Lett.*, 2020, **18**, 393–415.
- 38 A. A. Ichou, R. Benhiti, M. Abali, A. Dabagh, G. Carja, A. Soudani, M. Chiban, M. Zerbet and F. Sinan, Characterization and sorption study of Zn₂[FeAl]-CO₃ layered double hydroxide for Cu(II) and Pb(II) removal, *J. Solid State Chem.*, 2023, **320**, 123869.
- 39 S. K. Lagergren, About the Theory of So-called Adsorption of Soluble Substances, Kungliga Svenska Vetenskapsakademiens, *Handlinger*, 1898, **24**, 1–19.
- 40 G. Blanchard, M. Maunaye and G. Martin, Removal of heavy metals from waters by means of natural zeolites, *Water Res.*, 1984, **18**, 1501–1507.
- 41 H. N. Tran, S.-J. You, A. Hosseini-Bandegharaei and H.-P. Chao, Mistakes and inconsistencies regarding adsorption of contaminants from aqueous solutions: A critical review, *Water Res.*, 2017, **120**, 88–116.
- 42 I. Langmuir, The adsorption of gases on plane surfaces of glass, mica and platinum, *J. Am. Chem. Soc.*, 1918, **40**, 1361–1403.
- 43 H. Freundlich, Über die Adsorption in Lösungen, *Z. Phys. Chem.*, 1907, **57U**, 385–470.
- 44 Y. choi, Y. Kim, K. Y. Kang and J. S. Lee, A composite electrolyte membrane containing high-content sulfonated carbon spheres for proton exchange membrane fuel cells, *Carbon*, 2011, 49, 1367–1373.
- 45 M. Okamura, A. Takagaki, M. Toda, J. N. Kondo, K. Domen, T. Tatsumi, M. Hara and S. Hayashi, Acid-Catalyzed Reactions on Flexible Polycyclic Aromatic Carbon in Amorphous Carbon, *Chem. Mater.*, 2006, 18, 3039–3045.
- 46 G. J. Lumetta, S. I. Sinkov, J. A. Krause and L. E. Sweet, Neodymium(III) Complexes of Dialkylphosphoric and Dialkylphosphonic Acids Relevant to Liquid-Liquid Extraction Systems, *Inorg. Chem.*, 2016, 55, 1633–1641.
- 47 Q. Shu, A. Khayambashi, X. Wang and Y. Wei, Studies on adsorption of rare earth elements from nitric acid solution with macroporous silica-based bis(2-ethylhexyl)phosphoric acid impregnated polymeric adsorbent, *Adsorpt. Sci. Technol.*, 2018, 36, 1049–1065.
- 48 J.-H. Chen, W.-R. Chen, Y.-Y. Gau and C.-H. Lin, The preparation of di(2-ethylhexyl) phosphoric acid modified

- Amberlite 200 and its application in the separation of metal ions from sulfuric acid solution, *React. Funct. Polym.*, 2003, **56**, 175–188.
- 49 C. D. Smith, F. H. Foersterling and M. L. Dietz, Solvent structural effects on the solubility of bis(2-ethylhexyl) phosphoric acid (HDEHP) in room-temperature ionic liquids, *Separ. Sci. Technol.*, 2020, **56**, 800–810.
- 50 W. Wang, R. Y. Park, D. H. Meyer, A. Travesset and D. Vaknin, Ionic specificity in pH regulated charged interfaces: Fe³⁺versus La³⁺, *Langmuir*, 2011, 27, 11917– 11924.
- 51 B. V. Egorova, M. S. Oshchepkov, Y. V. Fedorov, O. A. Fedorova, G. S. Budylin, E. A. Shirshin and S. N. Kalmykov, Complexation of Bi³⁺, Ac³⁺, Y³⁺, Lu³⁺, La³⁺ and Eu³⁺ with benzo-diaza-crown ether with carboxylic pendant arms, *Radiochim. Acta*, 2016, **104**, 555–565.
- 52 D. Depuydt, A. Van den Bossche, W. Dehaen and K. Binnemans, Halogen-free synthesis of symmetrical 1,3-dialkylimidazolium ionic liquids using non-enolisable starting materials, *RSC Adv.*, 2016, **6**, 8848–8859.
- 53 B. D. Coday, T. Luxbacher, A. E. Childress, N. Almaraz, P. Xu and T. Y. Cath, Indirect determination of zeta potential at high ionic strength: Specific application to semipermeable polymeric membranes, *J. Membr. Sci.*, 2015, 478, 58–64.
- 54 B. Y. Spivakov, E. S. Stoyanov, L. A. Gribov and Y. A. Zolotov, Raman laser spectroscopic studies of bismuth(III) halide complexes in aqueous solutions, *J. Inorg. Nucl. Chem.*, 1979, 41, 453–455.
- 55 O. Horváth and I. Mikó, Spectra, equilibrium and photoredox chemistry of iodobismuthate(III) complexes in acetonitrile, *Inorg. Chim. Acta*, 2000, **304**, 210–218.
- 56 C. M. Babu, K. Binnemans and J. Roosen, Ethylenediaminetriacetic Acid-Functionalized Activated Carbon for the Adsorption of Rare Earths from Aqueous Solutions, *Ind. Eng. Chem. Res.*, 2018, 57, 1487–1497.
- 57 N. A. Thiele and J. J. Wilson, Actinium-225 for Targeted alpha Therapy: Coordination Chemistry and Current Chelation Approaches, *Cancer Biother. Rad.*, 2018, **33**, 336–348.
- 58 R. G. Pearson, Absolute electronegativity and hardness: application to inorganic chemistry, *Inorg. Chem.*, 1988, 27, 734–740.
- 59 R. G. Parr and R. G. Pearson, Absolute hardness: companion parameter to absolute electronegativity, *J. Am. Chem. Soc.*, 1983, **105**, 7512–7516.